Chapter 3
Kinetics, Dynamics and Yield of H_2 Production by HPB

Knowledge of the kinetics of H_2 production is a necessary step towards a thorough understanding of the mechanisms involved in the complex system of microorganisms' metabolic pathways in the substrate, including H_2-producing bacteria, electron shuttles and hydrogenase enzymes. For this reason, detailed kinetics can shed light on the dynamics of glucose consumption as well as on the evolution of bioH_2 using an enriched HPB biomass. In this chapter, after a general introduction to the kinetics model generally used in anaerobic processes and in particular for H_2 production, we will analyze the kinetics and dynamics of H_2 production utilizing glucose as substrate. The kinetics are studied by applying an experimental approach such as the *modified initial rate method* which experimentally determines the derivatives of substrate consumption as well as the H_2 production.

3.1 Kinetic Models

3.1.1 Microorganism Growth Model

Several models are used to describe the behaviour of microorganisms under different physical or chemical conditions such as temperature, pH, and so on. These models allow prediction of microbial activity and metabolic products, and the detection of critical steps of the production and distribution metabolites [1]. In order to build these models, growth has to be measured; bacterial growth (Fig. 3.1) often shows a phase in which the specific growth rate starts at a value of zero time and then accelerates to a maximal value (μ_{max}) in a certain period of time, resulting in a lag phase time (λ). In addition, growth curves contain a final phase in which the rate decreases and finally reaches zero, so an asymptote (A) is reached. When the growth curve is defined as the logarithm of the number of organisms plotted against time, the changes in growth rate result in a sigmoidal curve, with lag phase just after $t = 0$ followed by an exponential phase and then by a stationary phase.

B. Ruggeri et al., *BioH₂ & BioCH₄ Through Anaerobic Digestion*,
Green Energy and Technology, DOI 10.1007/978-1-4471-6431-9_3

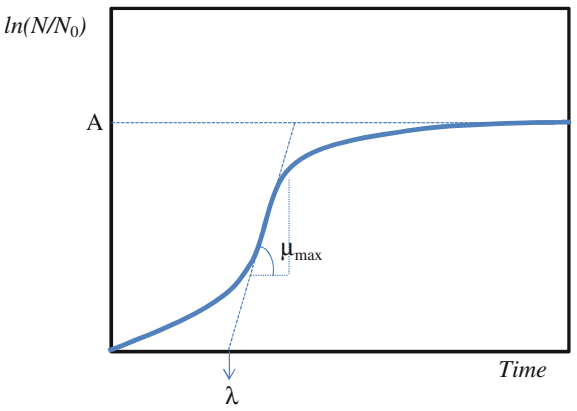

Fig. 3.1 A microorganism growth curve

A number of growth models are found in the literature, such as the models of Gompertz [2], Richards [3], Stannard et al. [4], the logistic model and others [5]. These models use as a variable only the number of organisms and do not include the consumption of substrate as a model based on the Monod equation would do. Besides the lag period and the asymptotic value, another valuable parameter of the growth curve is the maximum specific growth rate (μ_{max}). Since the logarithm of the number is used, μ_{max} is given by the slope of the line when the organisms grow exponentially. Usually this parameter is estimated by subjectively deciding which part of the experimental curve is approximately linear and then determining the slope of this curve section, eventually by linear regression. A better method is to describe the entire set of experimental data with a growth model and then estimate μ_{max}, λ and A by a best-fit procedure. Some authors indeed use growth models as those shown in Table 3.1 to describe their data. These models can describe the number of organisms (N) or the logarithm of the number of organisms [log(N)] as a function of time. The motivation for the decision to use a given model is usually not stated. Gibson et al. [7] found better results by a fitting procedure with the Gompertz model than other models.

Table 3.1 Some growth model used and their modified forms

Model	Equation	Modified equation
Logistic [6]	$y = \frac{a}{[1+e^{(b-cx)}]}$	$y = \frac{A}{\left\{1+e^{\left[\frac{4\mu_{max}}{A}(\lambda-t)+2\right]}\right\}}$
Gompertz [2]	$y = a \cdot e^{-e^{(b-cx)}}$	$y = Ae^{\left[-e^{\frac{\mu_{max}\cdot e}{A}(\lambda-t)+1}\right]}$
Richards [3]	$y = a\left\{1+v\cdot e^{[k(\tau-x)]}\right\}^{\left(-\frac{1}{v}\right)}$	$y = A\left\{1+v\cdot e^{(1+v)}\cdot e^{\left[\frac{\mu_{max}}{A}\cdot(1+v)\left(1+\frac{1}{v}\right)\cdot(\lambda-t)\right]}\right\}^{\left(-\frac{1}{v}\right)}$
Stannard et al. [4]	$y = a\left\{1+e^{\left[-\frac{(l+kx)}{p}\right]}\right\}^{(-p)}$	$y = A\left\{1+v\cdot e^{(1+v)}\cdot e^{\left[\frac{\mu_{max}}{A}\cdot(1+v)\left(1+\frac{1}{v}\right)\cdot(\lambda-t)\right]}\right\}^{\left(-\frac{1}{v}\right)}$

Since bacteria grow exponentially, it is often useful to plot the logarithm of the relative population size [$y = \ln(N/N_0)$] against time where N_0 is the number of microorganism at time $t = 0$ (Fig. 3.1). The three phases of the growth curve can be described by three parameters: the maximum specific growth rate μ_{max}, defined as the tangent in the inflection point; the lag time λ, defined as the x-axis intercept of this tangent; and the asymptote [$A = \ln(N/N_0)$]. Curves may show a decline; this kind of behaviour is called the death phase.

Most of the equations describing a sigmoidal growth curve may contain mathematical parameters (a, b, c …) rather than parameters with a biological meaning (A, μ_{max} and λ). It is difficult to estimate start values for the parameters if they have no biological meaning.

3.1.2 Kinetic Models of Anaerobic Processes

Substrate biodegradation, which occurs in a conventional anaerobic digester under the activity of several microorganism species, depends on the degree of activity of these microorganisms, in which the role of methanogens becomes limiting. The study of the process kinetics can be described by the kinetic models used for a monoculture, such as the model proposed by EI-Mansi [8] (Eq. 3.1), which is a saturation type on carbon source and where the growth is linearly dependent on the microorganism concentration:

$$r_x = \frac{\delta X}{\delta t} = \frac{\mu_{max} X \cdot S}{K_s + S} \tag{3.1}$$

where

r_x = bacterial growth rate;
X = concentration of biomass;
t = time;
μ_{max} = maximum specific growth rate;
S = limiting substrate concentration;
K_s = half saturation coefficient.

This model is applicable to the kinetic study of a bacterial population whose development is limited by only one substrate. Among several equations which relate the specific growth rate coefficient to the concentration of limiting nutrient, the Monod one is the most popular and usually fits actual data quite well. Considering the yield $Y_{X/S}$ defined as the ratio between the growth rate and the substrate consumption rate [9], it is possible to write that:

$$Y_{X/S} = -\frac{r_x}{r_s} = -\frac{X_0 - X}{S_0 - S} \tag{3.2}$$

where

X_0 = initial bacterial concentration;
S_0 = initial concentration of the substrate.

The following differential equation is generally used to include microbial growth and maintenance:

$$-\frac{\delta S}{\delta t} = Y_{X/S} \cdot \frac{\delta x}{\delta t} + m_s X \tag{3.3}$$

The first term on the right-hand side refers to substrate consumption for microbial growth, and the second one to microbial activity without growth, where m_s indicates the maintenance coefficient based on substrates consumed for energy purposes only. Equation (3.3) gives the rate of substrate disappearance in a system, in which the degradation kinetics is controlled only by the concentration of bacteria and the substrate. K_s is the value of substrate concentration corresponding to half the maximum specific growth rate of biomass. Thus, a low value of this parameter indicates the ability of microorganisms to easily assimilate the substrate. Most of the mathematical models explain the processes of anaerobic digestion by considering completely mixed systems, with or without recirculation of solids. Contois (1959) has proposed a different model based on the following kinetic equation [10]:

$$\mu = \frac{\mu_{\max} S}{(BX + S)} \tag{3.4}$$

where B is a constant kinetic parameter, and the saturation constant K_s does not appear. Equation (3.4) describes well the kinetics of systems with microbial growth limited by mass transfer, for example the digestion of animal wastes. Andrews (1968) developed a mathematical model for the processes of anaerobic digestion which considers the metabolism of volatile fatty acids (VFA) (including acetic and propionic acid) [11]. He introduced the concept of substrate inhibition in large concentrations, due to the presence of a fraction of non-ionized VFA whose concentration depends on the pH of the medium. Considering the non-ionized acids as substrate and expressing their limiting effect in the coefficients K_s and K_i, the following equation is a so-called inhibition growth kinetics model:

$$\mu = \frac{\mu_{\max} S}{(K_s + S)\left(1 + \frac{S}{K_i}\right)} \tag{3.5}$$

where

S = non-ionized substrate concentration and K_i = inhibition constant. Heyes and Hall [12] challenged this model by saying that the inhibition is not a function of non-ionized VFA; high concentrations of VFA are the result of substrate utilization and not the cause of the fermentation instability. They found that H_2 concentration could be a useful stability parameter. Instead, Mosey [13] considered the hydrogen

partial pressure as the key regulatory parameter of the anaerobic digestion of glucose, and hence he adopted it as a control variable because it affects the redox potential of the liquid phase. The relative production of VFA is assumed to be dependent on the redox potential or, equivalently, on the ratio [NADH]/[NAD^+] [14]. Lyberatos and Skiadas [14] concluded that the relationship between the reduced form and oxidized form of NADH controls the rate of conversion of propionic acid and butyric acid. Furthermore, they affirmed the existence of a direct relationship between the fraction NADH/NAD^+ and the partial pressure of hydrogen in the gas phase, using this relationship in an equation similar to that of Monod.

3.1.3 Some Kinetic Models for H_2 Production

To describe the progress of batch fermentative hydrogen production, several authors very often apply the *modified logistic equation* (Eq. 3.6) or *modified Gompertz equation* (Eq. 3.7) to estimate hydrogen production potential ($V_{gas,max}$), biogas production rate ($R_{max,gas}$) and lag phase (λ):

$$V_{gas} = \frac{V_{gas,max}}{1 + \exp[((R_{max,gas} \cdot e)/V_{gas,max})(\lambda - t) + 1]} \tag{3.6}$$

$$V_{gas} = V_{gas,max} \exp\left\{ - \exp\left[\frac{R_{max,gas} \cdot e}{V_{gas,max}} [\lambda - t] + 1 \right] \right\} \tag{3.7}$$

where V_{gas} is the total amount of H_2 produced (mL) at reaction time t (h), $V_{gas,max}$ is the potential maximal amount of H_2 produced, R_{max} (mL/h) is the maximum H_2 production rate, λ (h) is the lag phase to exponential biogas production and e is exp (1), i.e. 2.71828 [6].

The cumulative experimental data of H_2 production is described with Eq. 3.7 in order to estimate the three parameters $V_{gas,max}$, R_{max} and λ characterizing the experimental test. The parameters were estimated by employing a non-linear best-fit procedure. In addition, using $V_{gas,max}$ values and Eq. 3.7, the half period time (HPT) can be evaluated, which represents the time at which a quantity of H_2 equal to $V_{gas,max}/2$ was produced. HPT is a kinetic parameter, i.e. the time necessary to reach 50 % of the yield; it indicates the time at which the production rate is at its maximal value.

The Monod model is widely used to describe the effects of substrate concentration on the rates of substrate degradation, HPB growth and H_2 production. The Arrhenius model was used to describe the effect of temperature on fermentative H_2 production, while the modified Han–Levenspiel model [15] was used to describe the effects of inhibitors on fermentative hydrogen production. The Andrew model was used to describe the effect of H^+ concentration on the specific H_2 production rate, while the Luedeking–Piret model and its modified form was widely used to describe the relationship between the HPB growth rate and the product formation

rate [15]. Despite many kinetics studies in the literature, we noticed the lack of models which incorporate important parameters affecting hydrogen production, such as pH and redox, which influence enzymes involved in hydrogen production, such as ferredoxin (Fd) and hydrogenase. Therefore, the aim of the following sections is to suggest a macro-approach methodology to set up a formal kinetics of H_2 evolution. To this end the kinetics of bio-hydrogen production on glucose by HPB culture was set up and described, taking into consideration the structural information on the enzymes involved in hydrogen production.

3.2 Experimental Section

3.2.1 HPB Sewage Sludge Enrichment

The anaerobic microorganisms used in this study were withdrawn from an anaerobic digester of a municipal wastewater treatment plant. The pH, density, volatile solid (*VS*) and total solid concentration (*TS*) of the sewage sludge used were 7.3, 1,010 g/L, 10,875 and 14,500 mg/L respectively. The sludge was pretreated as described in Chap. 2. To avoid differences between the tests, all the seeds came from the same pretreatment batch. At the end of treatment, the sludge was divided in several portions of 50 mL and each of them was frozen. Before inoculation the seed was thawed at ambient temperature and then gently heated to the working temperature.

3.2.2 Fermentation Tests

Kinetic studies were carried out in 500 mL (450 mL working volume) Erlenmeyer flasks, agitated daily, and flushed at the beginning with nitrogen gas for 5 min in order to remove air from the system. The treated sludge was used as seed in the ratio of 10 % v/v. Initial glucose concentration values tested in batch condition were 5, 25, 45, 60, 70 and 90 g/L. The composition of the medium was formulated by adding micronutrient solution [16] in order to reach an initial C/N ratio of about 30. The initial pH of the media was set in the range 6.6–7.4 by using 2 N NaOH solution. Tests were conducted at 35 ± 1 °C in a thermostatically controlled room; each measurement is the result of a triplicate test. Tests were stopped when the biogas production shut down.

A single test was conducted in a 2 L bioreactor (Minifors, Infors AG, Switzerland) under the following conditions: 60 g/L of glucose and micronutrients as above, agitation of 100 rpm and ambient temperature of 22–28 °C. The initial pH was 7.3; pH was readjusted to 6 using 2 M NaOH solution when gas production shut down at 60 h of fermentation time and when pH reached 4.4 at 150 and 190 h of fermentation time.

3.2.3 Analytical Methods

Gas evolution in the tests conducted in Erlenmeyer flasks was monitored during the fermentation by the water-replacement method, its composition was measured at the end of the lag phase (≈10 h) and at the end of fermentation, and an average value was obtained. At the end of fermentation, the concentrations of ethanol and acetic, propionic and butyric acids were also detected. During the tests, liquid samples were withdrawn in order to measure pH and redox potential. Gas composition was measured by gas chromatography (Varian CP, 4900) equipped with a thermal conductivity detector (TCD); pH was measured by a pH meter (Infors AG, Switzerland); redox potential was measured by a Pt4805-DXK-S8/120 electrode (Mettler Toledo, Switzerland). Glucose concentration was measured by enzymatic bio-analysis (Biopharm-Roche). The concentrations of ethanol and acetic, propionic and butyric acids were detected by a gas chromatograph (Model 6580, Agilent Inc., USA) equipped with a flame ionization detector (FID).

3.2.4 Kinetics Study

3.2.4.1 Modified "Initial Rate Method"

Gas production rate was evaluated by linear regression of experimental values of the volume of total gas produced per unit reaction volume during the exponential phase; glucose uptake rate was evaluated by linear regression of experimentally determined concentrations during the same exponential phase. This is a type of *initial rate method* usually employed for enzymatic reactions [17], considering as negligible the variation of limiting and inhibiting effects on the measuring range. In the present case the derivative time period starts after a lag phase of about 20 h. The initial rate method involves measuring the rate of reaction at very short times, before any significant change in concentration occurs. During the exponential phase biogas production and glucose uptake rates show a linear behaviour with time until a sharp pH effect (drop to pH 4.3) that shuts down fermentation; this confirms the initial rate method hypotheses. Uncertainty was estimated to be around 20 % as standard deviation on the repeated tests.

3.2.4.2 Data Analysis

Gas production rate and glucose uptake rate were best fitted against average glucose concentration during the exponential phase. Several kinetic models were considered for gas production to fit the experimental data; they are reported in Table 3.2. Instead, linear best fit was used for glucose uptake rate; the R^2 value was taken into account in order to choose the kinetic model. The statistically low number of experimental data limits the R^2 values.

Table 3.2 Biogas kinetic models used to best fit experimental data

Equation	R^2
$r(P) = \frac{r_{max} S}{K_S + S}$	0.71
$r(P) = \frac{r_{max} S}{K_S + S + S^2/K_I}$	0.81
$r(P) = \frac{r_{max} S}{K_S + S} \exp(-S/K_1)$	0.82
$r(P) = aS + bS^2$	0.88
$r(P) = aS + bS^2 + cS^3$	0.94

3.3 Results and Comments

The shape of the fermentation line against time is similar for all the glucose concentrations tested and presents four phases, during which different behaviours are observed. Figures 3.2, 3.3 and 3.4 report the values of gas production as volume per unit reaction volume, glucose concentration, measured pH and redox values against fermentation time, for the lowest, the highest and the intermediate glucose concentrations tested, respectively. There are four fermentation phases, as mentioned previously:

1. During the first 18–22 h the gas production rate was very low in all the tests, ranging between 2 and 7 mL/Lh; no hydrogen was measured in the gas produced in this period. Table 3.3 reports the variation of the measured variables at 10 h of fermentation.

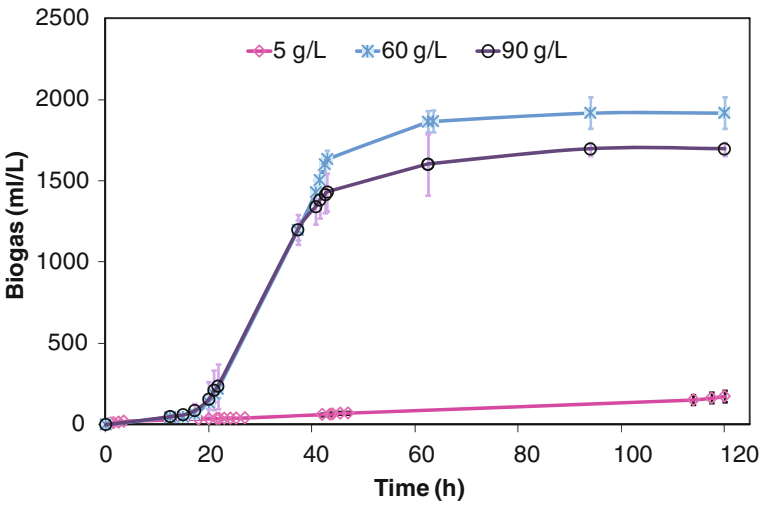

Fig. 3.2 Biogas production versus time in low (5 g/L), medium (60 g/L) and high (90 g/L) glucose concentration tests

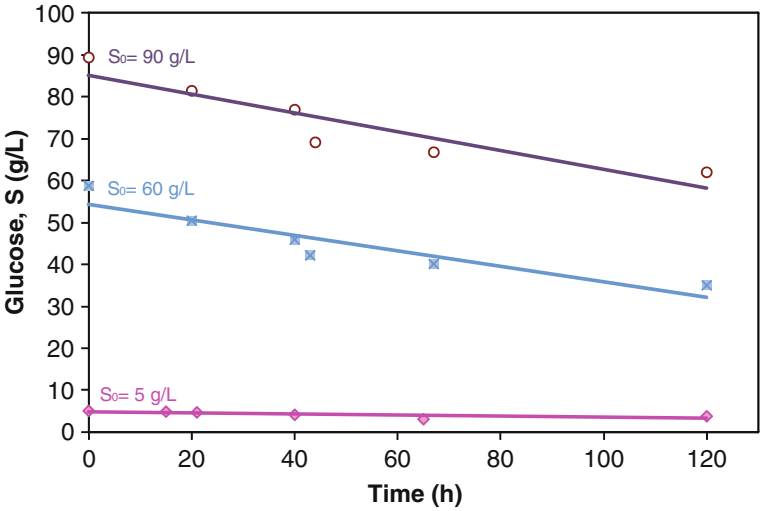

Fig. 3.3 Glucose concentration variation versus time in low (5 g/L), medium (60 g/L) and high (90 g/L) glucose concentration tests

2. At 18 h of fermentation the gas production rate increased sharply to 10–100 mL/Lh depending on initial substrate concentration; the values reached were maintained up to pH values of 4.2–4.4 after around 30–40 h of fermentation.
3. When the pH reached 4.2–4.4, the gas production rate decreased sharply in all the tests; biogas shut-down occurred when the pH was in the range 3.2–4.0.
4. After the gas production stopped, glucose continued to be consumed at a reduced rate until the complete arrest of fermentation.

The gas production rate has different values in the four phases; during the first two phases it is constant. The measured glucose uptake rate shows similar values in the first three phases and slows down in the fourth one. pH decreases in all the phases, much more rapidly during the first (Fig. 3.4). Redox potential decreases during the first phase, and falls at the end of the first phase to between –400 and –500 mV; it increases very slowly during the exponential phase and increases strongly during the third phase, reaching a value in the range –100 to –300 mV. The redox behaviour in the test at very low glucose concentration (5 g/L) does not show an increase during the exponential phase. During the first phase gas production is in a lag phase, during the second phase gas production is in an exponential phase (i.e. medium composition changes do not affect hydrogen production), during the third phase hydrogen production is inhibited by the low pH values, and during the fourth phase gas production is completely stopped by the low pH values. The main experimental results are reported in Table 3.4.

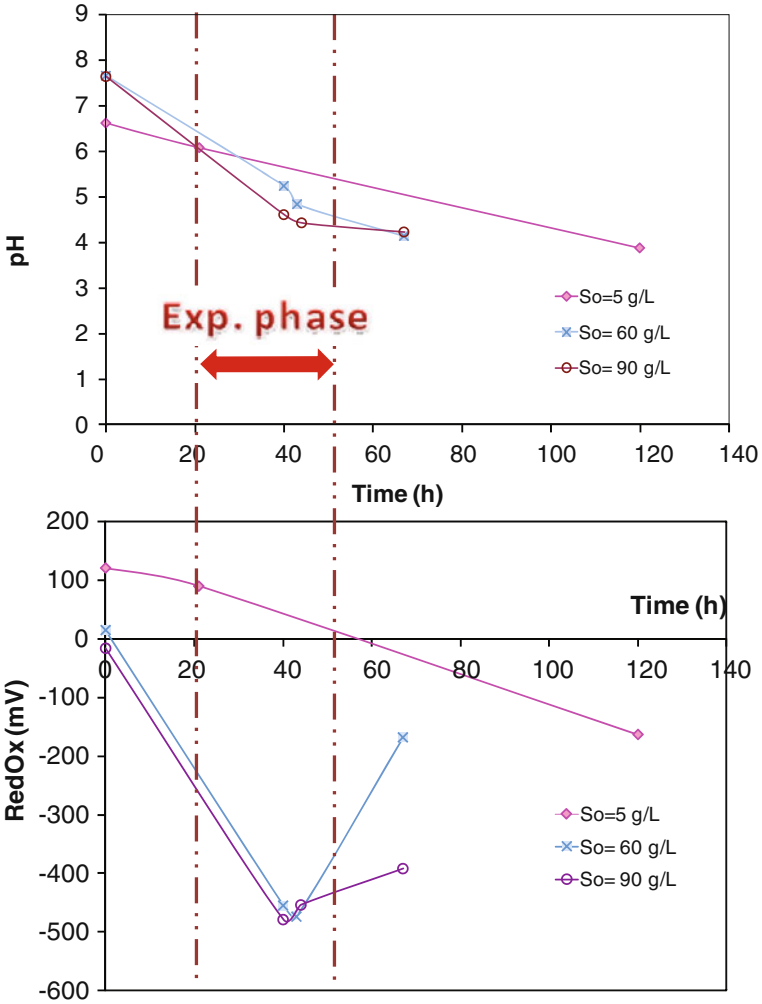

Fig. 3.4 pH and redox versus time

3.3.1 Lag Phase

During the first period the microorganisms were active but there were not yet favorable conditions for hydrogen evolution. Although pH and redox are reduced during the lag phase, pH remains in the neutral range (pH > 6.5) and redox remains in the low reductive range (redox > –200 mV). Several phenomena occur during the lag phase owing to the presence of different bacterial species. Facultative bacteria can evolve their metabolism towards the biosynthesis of ethanol, e.g. *Klebsiella pneumoniae*, which is able to produce in anaerobic condition either ethanol from

Table 3.3 Experimental results at 10 h of fermentation

Parameters	Nominal glucose concentration of tests					
	5 g/L	25 g/L	45 g/L	60 g/L	70 g/L	90 g/L
Glucose (g/L)						
t = 0 h	5.05	24.61	45.00	59.76	67.45	89.41
ΔS	0.18	0.79	1.5	2.2	2.80	2.70
Biogas (mL/L)						
t = 10 h	54	62	59	59	69	59
H_2 (%)	0	0	0	0	0	0
pH						
t = 0 h	6.61	6.64	7.28	7.29	7.07	7.37
ΔpH	−0.32	−0.24	−0.35	−0.48	−0.3	−0.52
Redox potential (mV)						
t = 0 h	121	70	80	−47	−10	15
Δredox	−12	−90	−110	−103	−107	−98

Table 3.4 Volume and composition of biogas produced and glucose utilization

Runs (g/L)	Biogas produced (mL/L)	H_2 (%)	CO_2 (%)	ΔS (mmol)	$\Delta S/S$ (%)
5	112 ± 7	60 ± 1	40 ± 1	7.2	25
25	600 ± 150	58 ± 2	42 ± 2	8.2	33
45	630 ± 170	60 ± 1	40 ± 1	49.8	20
60	1,920 ± 100	47 ± 12	53 ± 12	103.7	32
70	1,220 ± 210	58 ± 2	42 ± 2	105.6	28
90	1,700 ± 40	40 ± 12	60 ± 12	125.6	25

glucose or acetic acid from acetyl-CoA [18]. Following the ethanol metabolic pathway, all NADH produced is consumed; in other words the ethanol biosynthesis pathway is in full competition with metabolic products that are coupled with NADH regeneration for biogenesis of H_2, for example. Acetic acid is produced in low quantities, reducing pH and lowering the redox until *Clostridium* spp. are able to activate the acetic and butyric pathways to produce H_2. The production of molecular hydrogen maintains the electron balance in which protons act as electron acceptors and the substrate acts as electron donors [19], as shown in Chap 1. This can occur only if an adequate difference in electrical potential exists as the driving force, i.e. redox needs to be at an adequate value. Glucose uptake generates ATP, NADH and NADPH through the glycolysis pathway and oxidative decarboxylation of pyruvate. NADH and NADPH, in anaerobic conditions, need to be oxidized to NAD^+ and $NADP^+$ for cellular activity. The reoxidation processes are activated by iron–sulfur proteins that act as electron donors in many systems, interacting with flavoproteins, hemoproteins and other more complex iron–sulfur proteins. For *Clostridium* spp. it is well accepted that structural proteins such as Fd are able to transfer electrons to H^+ mediated by the hydrogenase enzyme, whereas the action of

[Fe]-Fd-hydrogenase is to remove excessive reducing equivalents during fermentation by strictly anaerobic bacteria such as Clostridia [20]. [Fe]-Fd-hydrogenase is an active oxidation–reduction group in the chain which transfers electrons from carbohydrates to protons able to generate hydrogen via pyruvate synthesis in anaerobic acetogenic bacteria [17]. The key point to be considered is that the Fd forms a complex such as Fd · Fd $NADP^+$ reductase, found in *Clostridium acetobutylicum* [21]. The interactions between Fd and the complex are strongly affected by the pH of the medium. At near-neutral pH values (6–7) a proton is taken up when Fd and Fd·$NADP^+$ reductase form a complex. The complex dissociation constant depends on pH: for pH > 8.5 the Fd is all in the complexed form, while for pH < 8.5 free Fd appears; this suggests that the redox potential of Fd is strongly affected by the pH value. In other words when the pH decreases more the Fd is free and its redox shifts toward its reductive value of –425 mV [21]. Thus the lowering of pH creates a reductive environment (Fd acts as electron donor), while high pH creates an oxidative environment (Fd acts as electron acceptor). Free Fd is predominantly in the oxidized form (Fd^{3+}) and presents a lower capacity to act as electron donor to protons via hydrogenase to form hydrogen. In such conditions, electrons produced by the oxidation of pyruvate to acetyl-CoA are used to produce alcohols and lactate instead of hydrogen. The lowered reducing power of Fd·$NADP^+$ reductase is probably not used to form molecular hydrogen as the terminal electron acceptor; on the contrary, part of the reduced Fd produced is used to generate NADH, which mitigates against hydrogen production. Uyeda and Rabinowitz [22] demonstrated that low-potential electron donors, like reduced Fd, can drive the reductive carboxylation of acetyl-CoA. Moreover it is well known that *Clostridium* spp. do not grow well at pH < 5 [22], as verified also in the present study, and at high glucose concentrations. Other researchers detected the production of ethanol and butanol in experiments using mixed sludge from municipal wastes [23], as occurs in the case of the facultative bacteria *Klebsiella pneumoniae* [18]. Hence one can argue that in the lag phase there is a low activity of the HPB, due to the presence of facultative microorganisms, which take advantage of the presence of micro aeration zones in the broth. Therefore, the metabolic pathways are oriented towards the formation of metabolites other than hydrogen due to the difficulties in Fd and hydrogenase transferring electrons owing to the high value of pH and redox. During the lag phase pH decreases slightly while redox remains at very slightly reductive values (refer to Table 3.3). From this analysis, we suggest that in the lag phase the biomass activity was probably oriented to organize the "environment" to allow *Clostridium* spp. to activate hydrogen production. At the end of the lag phase a metabolic shift occurs and the redox value rapidly decreases to reach values ranging between –400 and –550 mV, enabling reoxidation of NADH and NADPH with hydrogen that acts as an electron acceptor (refer to Fig. 3.4). In order to highlight the experimental evidence, it is important to recall the metabolic pathway of glucose. Owing to the presence of a microorganism consortium it is impossible to refer to such a specific pathway of glucose. Bearing in mind the origin of the biomass used, one can agree that, at least, the following species might be present: *Escherichia, Salmonella, Shigella, Klebsiella, Enterobacter* [24] and, obviously,

Clostridium spp. All the species present are able to activate acid fermentation with the possibility of an alcoholic fermentation too. Figure 1.7 of Chap. 1 depicts a "virtual" metabolic pathway of glucose which accounts for the main microorganisms present in the HPB culture able to produce metabolites such as acetic, propionic, ethanol and butyric acids, the biomass itself and H_2 and CO_2.

Chen et al. [25] observed that *C. butyricum* on sucrose started to produce hydrogen at the end of the exponential growth when the microorganisms had entered an early stationary phase. This means that, during the lag phase, glucose is mainly consumed for biomass growth. Thus, one can suppose that during the lag phase electrons mainly flow toward biosynthesis and are not used for hydrogen evolution. The reason for this behaviour remains to be explained.

3.3.2 Exponential Phase

The second phase starts at around the 20th hour of fermentation. During this phase the gas production rate and glucose uptake rate are constant (Figs. 3.2 and 3.3). The duration of the exponential phase is different for each test, ranging from 10 to 30 h. It ends when pH goes below a threshold; the comparison of Fig. 3.2 with Fig. 3.4a on the time axis shows that biogas evolution starts when the pH of the medium reaches a value of approximately 6.5 and continues while the pH remains over 4.5. As reported above, the lowering of the pH provokes an increase of free Fd, shifting the redox potential towards reductive values. For the production of H_2 it is necessary that the [Fe] · Fd · hydrogenase complex donates an electron to a proton. Hydrogenase in H_2 production has been studied for several decades [26]; in particular Chen and Blanchard discovered a second hydrogenase (hydrogenase II) in *C. pasteurianum* in addition to hydrogenase I, with the presence of two [8Fe–8S] clusters able to activate the redox reaction. Hydrogenase II as well as hydrogenase I is able to evolve H_2 with Fd as the sole electron carrier. Adams and Mortenson [27] studied the physical and catalytic properties of hydrogenase II compared with hydrogenase I, in particular the pH effect on hydrogenase that catalyzed H_2 evolution. Hydrogenase I has maximal efficiency at pH 6.3, hydrogenase II has maximal efficiency at pH 5.8 and at pH < 5 the activity of both the enzymes decreases rapidly. It is interesting to note that during the exponential phase pH ranges between 4.4 and 6.5 (Figs. 3.1 and 3.3a), while at pH 5 *Clostridium* spp. activity shuts down [25]. The above considerations suggest that the role of pH in the production of H_2 is strongly linked with hydrogenase activity. The positive effect as a consequence of pH decrease is the release of Fd from the complex Fd · $NADP^+$ reductase, which creates a more reductive environment and the formation of an optimal spatial conformation of hydrogenases I and II with a maximal activity of the enzyme pool, as also reported in Chap. 2. The increase in redox potential during the exponential phase (Fig. 3.4b) indicates that in the medium the availability of electrons decreases because the system moves towards a less reductive range.

All these considerations clearly provide evidence, from an engineering point of view, of the necessity to strictly control the pH in the reactor, in order to prevent the pH going below the 6.2–5.4 range; this can be achieved by addition of NaOH.

3.3.3 Kinetics Evaluation

Gas production rate and glucose uptake rate, experimentally evaluated in the exponential phase, were best-fitted against glucose average concentration. As stated previously, several kinetics models were considered for gas production to fit the experimental data reported in Table 3.2. Gas production rate shows a limitation at low substrate concentration and an inhibition at high substrate concentration. No theoretical findings help in choosing one kinetics model among others; hence the best-fit criterion was used to select the regression model. Substrate inhibition is sharper than either the Haldane or exponential models can handle; hence a polynomial of third degree is necessary to reach an acceptable statistical correlation (R^2 value) (Table 3.2). Gas production rate data experimentally evaluated on exponential ranges and the model curve are shown in Fig. 3.5 along with the experimental uncertainty affecting the data. The maximum production rate of over 100 mL/Lh is reached at a glucose concentration below 60 g/L. Experimental data and the regression curve for glucose kinetics are shown in Fig. 3.6. A linear first-order kinetics was set up and a best fit was used for glucose uptake rate; an R^2 value of 0.94 was obtained.

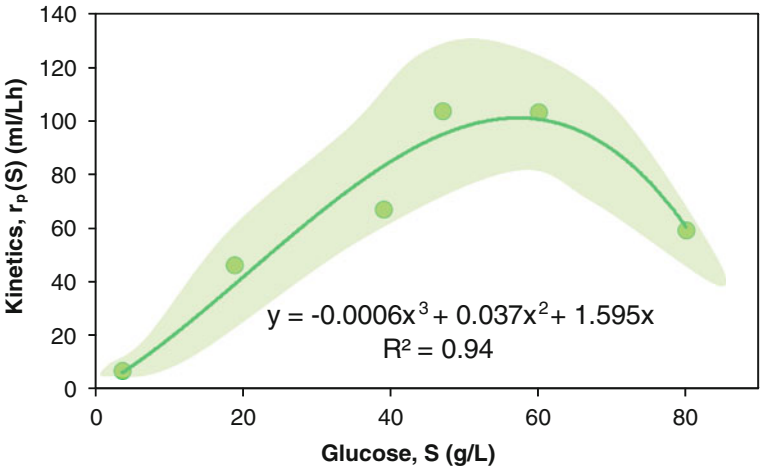

Fig. 3.5 Kinetics of biogas production rate with area of experimental uncertainty

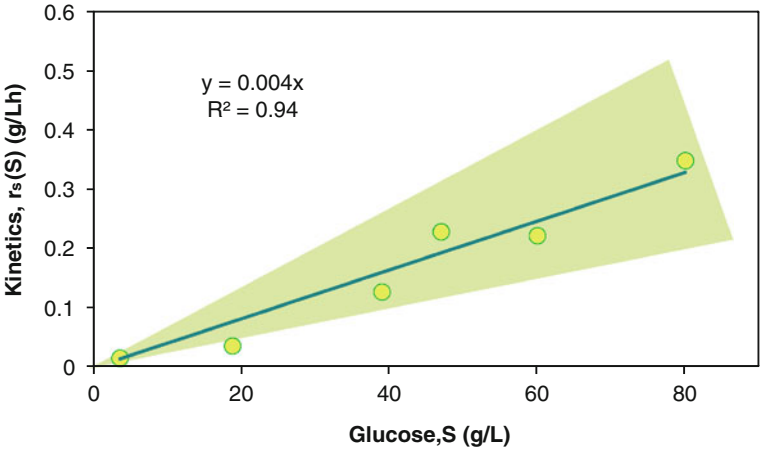

Fig. 3.6 Kinetics of glucose consumption rate with area of experimental uncertainty

The difference between the kinetics of glucose consumption and biogas evolution is not a surprise, owing to the use of the unstructured modeling approach [28] that allows a good reference model for the design of a reactor and prediction of the system dynamics.

3.3.4 Dynamics of bioH_2 Evolution

Using the kinetics equations evaluated, this section aims to highlight the system dynamics by a macro-approach [29]. In analyzing such a complex system, as schematized in Fig. 1.7, a reduction of complexity is necessary. The aim of a macro-approach analysis is to find the controlling phenomenon which determines the dynamics of the whole system. To find the controlling step, using the terminology of chemical reaction engineering, it is necessary to put the macro-phenomena, i.e. observable, experimentally detectable phenomena, on the time axis using a relaxation time parameter [30]. A macro-schematization of pathways of Fig. 1.7 is shown in Fig. 3.7, according with the experimentally detected parameters. Three macro-phenomena can be defined and the corresponding *relaxation time* (see Appendix) must be evaluated:

1. Glucose uptake producing electrons by the following macro-reaction:

$$\text{glucose} \rightarrow \text{pyruvate} + e^- \tag{3.8}$$

2. Proton production generating the variation in the pH in the broth by the following macro-reaction:

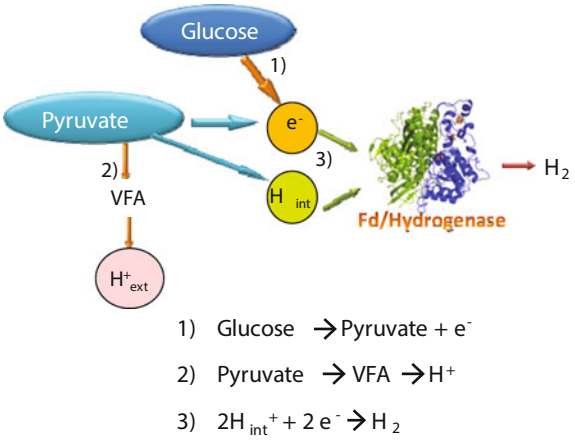

Fig. 3.7 Macro-approach to dynamics of H_2 evolution by HPB

$$\text{pyruvate} \rightarrow \text{VFA} \rightarrow \text{H}_{\text{ext}}^{+} \tag{3.9}$$

3. Hydrogen production experimentally detected by biogas evolution by the following macro-reaction:

$$2\text{H}_{\text{int}}^{+} + 2\text{e}^{-} \rightarrow + \text{H}_2 \tag{3.10}$$

The reactions (3.9) and (3.10) proceed in parallel and in series to (3.8). Evidence of this comes from the experimental tests reported in Chap. 4 conducted with continuous pH control with NaOH: during H_2 evolution a concurrent consumption of the base occurs. This suggests that two different locations of proton are present. It is important to remark that serial reactions are controlled by the slowest reaction while parallel reactions are controlled by the most rapid reaction. It is necessary to clarify that the above reactions are only a macro-schema in order to link the experimentally measured macro-parameters with such mechanisms. The protons of reaction (3.9) and (3.10) are topologically different: the first type is external of the cell machinery and is responsible for the pH variation occurring in the broth, while the second type is inside the cell and can be transformed into H_2 gas via hydrogenase activity and hence detected as hydrogen gas.

For each of the above macro-reactions, it is possible to estimate the respective relaxation time. For glucose uptake a first-order kinetics was observed, and thus the relaxation time is a constant:

$$\tau_{Gl} = 1/K \tag{3.11}$$

For bioH_2 production a non-linear kinetics was observed, and hence the relaxation time depends on substrate concentration; it can be estimated using the following equation [30]:

$$\tau_P = [r_P(S)/S]^{-1} \tag{3.12}$$

For H^+ production, the relaxation time τ_{H+} was estimated from the experimental pH values following the definition of relaxation time [30], i.e. the relaxation time is the value of time corresponding to 63 % (1 – 1/e) of the observed variation from initial to final H^+ concentration. The relaxation time of the three macro-reactions versus glucose concentration is shown in Fig. 3.8. The range of substrate concentration tested can be divided into two main parts: part A in which the production of electrons is the controlling step, and which occupies almost the whole range of glucose concentration investigated; part B, at very low glucose concentrations (<10 g/L), where the release of H^+ in the medium becomes the slowest phenomenon, i.e. the H^+ formation is the limiting step of the microbial activity. Part A may be divided into two zones: zone A_1 where the production of protons is the faster phenomenon: $\tau_{H+} < \tau_P$, i.e. the dynamics is controlled by the pH decrease and an accumulation of electrons occurs, together with a modification of the environment towards a more reductive electrical potential; and zone A_2 where bioH_2 production becomes the faster phenomenon: $\tau_{H+} > \tau_P$, i.e. the dynamics is governed by the change in the rate of decrease of pH, because the protons generated by reaction (3.9) are partially consumed and a surplus of available electrons occurs. This creates a shift towards a more oxidative potential, because when the hydrogen is produced the redox moves into a more positive range against the H_2 reference electrode. In part B at low glucose concentration in which the controlling step becomes the pH variation ($\tau_{H+} > \tau_{Gl} > \tau_P$), the overall reaction proceeds very slowly owing to the difficulty of the microorganisms in changing the pH for endogenous phenomena only, i.e. low production of "free" protons.

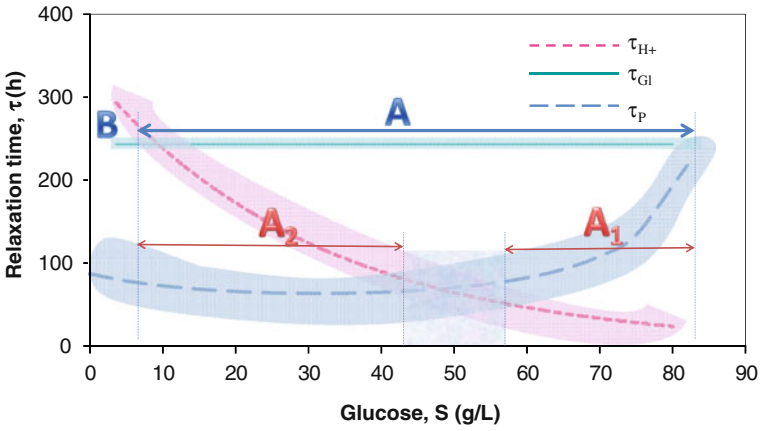

Fig. 3.8 Relaxation time estimation of macro-reactions

The above evaluation of the dynamics of H_2 production deserves some important suggestions for scale-up purposes. In the range A_1, where the biological system is controlled by the pH variation (towards the acid range) it is most important to have very efficient pH control (probe, controller and actuators). Considering that this occurs at high glucose concentration, which means high viscosity of the fermenting broth, the major role belongs to the mixing system. In the range A_2, at low glucose concentration, the biological process is governed by H_2 production, which can inhibit the bioreaction (Chap. 1), hence it is important to favor the degassing of the broth in order to lower the amount of H_2 gas dissolved in it. This can be controlled by increasing the mixing of the broth. In conclusion, the mixing of the fermenting broth is a fundamental parameter to consider in the scaling up of such a bioH_2 production bioreactor.

This analysis is valid for the exponential phase because the kinetics is evaluated in this range; nevertheless, in our opinion, in the light of the above dynamic considerations, the apparently strange behaviours of pH and redox reported in Fig. 3.4a, b are elucidated. In fact, in all the tests (initial glucose concentration >10 g/L) the pH presented two rates of variation and the redox shown a decrease toward reductive values; when biogas evolution occurs in the exponential phase, redox quickly moves toward the oxidative range. Recalling the structural considerations about the spatial configuration of Fd and hydrogenase I and II as pH-dependent, one could argue that the dynamic analysis and activities of enzymes are coherent. This is thanks to the macro-approach, even if it presents a low degree of precision but a good degree of exactness in the Zadeh sense [31]. The above dynamics gives an explanation of the different behavior of pH and redox versus time, as a monotonic curve appears for the test using 5 g/L of glucose (Fig. 3.4); the fermentation progress is always under H^+ production, which is the limiting step. Lastly, the above comments on the dynamics of H_2 evolution suggest the necessity to have an external pH control at high glucose concentrations (>5–8 g/L) in order to shift the reoxidation of NADH and NADPH toward H_2 gas formation via Fd and hydrogenase enzymes pools, as experimentally verified.

3.3.5 Test in Bioreactor

In order to check the robustness of the dynamical considerations, a fermentation test using a bioreactor with external (no endogenous) pH variation was done. The test was conducted at an initial glucose concentration of 60 g/L and the seed (10 % v/v) was acid-pretreated in the same way as each test presented in this chapter. Figure 3.9 shows the behavior of the fermentation over time: after the “natural” decrease, pH was varied three times by adding NaOH in order to reach the range of optimal enzyme activity (6.8–5.4). In all cases the redox was lowered and biogas evolution restarted, though with a different rate. The test demonstrates, in the authors’ opinion, the validity of the kinetics and dynamics considerations supported by the spatial structural role of Fd and hydrogenase I and II. In particular, from

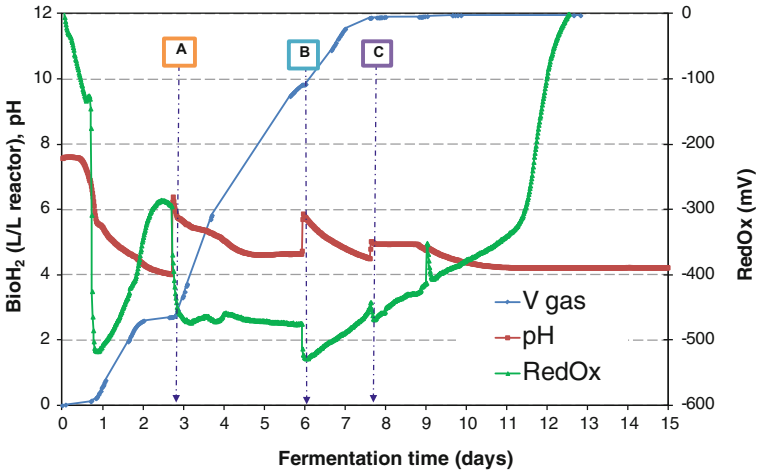

Fig. 3.9 Test on bioreactor: glucose, bioH_2, pH and redox versus time. *A*, *B* and *C* are points of pH restoration in the optimal range. Operative conditions are: 60 g/L glucose, (23–28) °C working temperature, 100 rpm mixing rate, 10 % v/v seed HPB

Fig. 3.9, at each pH adjustment the increase in pH provoked a decrease of redox, although this effect was not of the same magnitude. This fact might be due to the incompletely reversible spatial structure of the enzymes. The elucidation of this aspect deserves additional attention and needs more detailing from theoretical as well as experimental point of views.

Regarding bioH_2 production, a comparison between the flask and bioreactor tests can be made almost 3 days before pH adjustment and at the same initial glucose concentration (60 g/L). During this time the only difference is agitation, and an increase in biogas production in the bioreactor test is observable. The quantification of this effect is reported in Sect. 3.3.6. As shown in Fig. 3.9, the pH control increases total biogas production about six-fold. This aspect confirms all the considerations reported in Sect. 3.3.4.

3.3.6 Yield

The effectiveness of such a bioreaction is an important parameter for evaluating the process and the operative conditions to be adopted; to this end a theoretical maximum reference yield needs to be defined. In the presence of mixed microorganisms and considering the complex pathways for the production of several VFA, the evaluation of the theoretical H_2 yield is doubtful, due to the fact that some bacteria consume H_2 while others produce alcohols and/or lactic acid, and other bacteria produce H_2 simultaneously with VFA production [32]. Considering the stoichiometry of hydrogen production from glucose, there are three main global reactions:

$$C_6H_{12}O_6 + 2H_2O \rightarrow 2CH_3COOH + 2CO_2 + 4H_2 \quad (3.13)$$

$$C_6H_{12}O_6 + 2H_2 \rightarrow 2CH_3CH_2COOH + 2H_2O \quad (3.14)$$

$$C_6H_{12}O_6 \rightarrow CH_3CH_2CH_2COOH + 2CO_2 + 2H_2 \quad (3.15)$$

They account for the acid formation metabolic pathway coupled with hydrogen formation. Bearing in mind that each metabolic product is coupled with different stoichiometric H_2, the question of how to take into account the differences in moles of hydrogen produced per moles of compound needs to be solved in order to evaluate the yield of H_2 relative to 1 mol of carbon source. To overcome the above question, the authors suggest experimentally evaluating the quantities of the metabolites and consequently correcting the stoichiometric yield for each compound and finally finding a theoretical reference yield value using the following equation:

$$Y^* = \sum_j^m Y_j * w_j \quad (3.16)$$

The reference yield (Y^*) means the maximum H_2 production per mole of glucose; Y_j is the stoichiometric H_2 yield for every *j-m* compound and w_j is the weight determined experimentally in reference to the total quantities of VFA and ethanol, disregarding the weight of other metabolites because of their low concentrations. Equation (3.16) has the advantage of linking Y^* to the specific fermentation, i.e. the quality of carbon source and the microbial consortium.

Table 3.5 shows the application of the suggested procedure: w_j is experimentally evaluated as the mean value obtained for all tests at the end of fermentation reported in Sect. 3.2.2. Its variability is about 10 %. The reference H_2 yield (Y^*), valid only for the actual fermentation, is equal to 1.66 mol H_2/mol of glucose. This value represents again a maximum theoretical value because of the difficulty in evaluating the quantity of glucose consumed, either for cellular growth or to produce other metabolites. The cellular growth is difficult to evaluate with precision because the total suspended solids in the feed at the start masks the biomass growth itself. The

Table 3.5 Experimental evaluation of the theoretical reference yield of H_2 per mole of glucose relative to mixed microorganisms

Compounds	Stoichiometric yield (mol H_2/mol glucose)	Mean distribution w_j (%)	Y_j (mol H_2/mol glucose)
EtOH	0	10.37	0.00
Acetic acid	4	3.56	0.14
Butyric acid	2	81.08	1.62
Propionic acid	−2	5.00	−0.10
Reference yield Y^*			1.66

Table 3.6 Effectiveness of H_2 production as ratio of actual yield Y_a to reference yield Y^* for all the experimental tests

Tests (g/L)	Y_a (mol H_2/mol glucose)	$\xi = Y_a/Y^*$ (%)
5	0.41	0.25
25	0.34	0.20
45	0.34	0.20
60	0.38	0.23
70	0.30	0.18
90	0.24	0.14
Bioreactor 60		
Before pH adjustment	0.49	0.30
At the end of fermentation	1.07	0.64

quantitative measure of the microorganisms involved in the H_2 production in presence of the HPB consortium, in our opinion, remains an open question from the experimental point of view in order to have an acceptable precision of the measure. Lastly, the effectiveness value ξ, the ratio between the actual Y_a determined experimentally and the reference yield Y^* as a measure of the efficiency of the fermentation, are reported in Table 3.6.

The comparison of the effectiveness of the test carried out in the bioreactor with external pH adjustment and the test with endogenous pH adjustment shows an increase in H_2 production of 2.8 times for the same initial glucose concentration of 60 g/L of Table 3.6. Nevertheless not all this increase can be attributed to pH variation because the test conducted with the bioreactor shows a degassing effect which leads to a higher Y_{H_2} due to agitation. In fact, the evaluation of the effectiveness at 65 h, i.e. before the first pH adjustment, gives a value of $\xi = 0.30$.

Comparing these results with that of $\xi = 0.23$ at an initial glucose concentration of 60 g/L, one can see that the effect of agitation causes an increase in effectiveness of 30 %, while the effect of pH adjustment increases the efficiency more than 100 %. Again, this experimental evidence confirm the dominant role of mixing in the scale-up procedure of bioH_2 production.

3.4 Conclusion

In the present Chapter a detailed kinetics was set up for glucose consumption as well as for biogas evolution using an enriched HPB biomass. The glucose consumption was found to be of first-order kinetics while for the biogas evolution an inhibited kinetics appeared over 60 g/L of glucose with a maximum production rate of around 100 mL/Lh. The H_2 content ranged from 40 to 60 %; this suggests that a full-scale application should have a carbohydrate concentration below 60 g/L in the fermenting broth. The positive effect of mixing was highlighted, as this is able to degas the biogas dissolved in the medium, consequently increasing H_2 production.

This effect could be estimated at around 30 %, in other words the present kinetics represents a conservative estimate of H_2 production from a quantitative point of view. The kinetics was used to highlight the dynamics of the biogas evolution using a macro-approach and relaxation time tools, to explain the experimentally detected behavior of pH and redox during the tests. Taking into consideration the behavior of the Fd and hydrogenase enzyme pools in the electron transfer chain, the dynamics appears to be coherent. In particular, pH seems to be the most important parameter in the regulation of the enzyme pool involved in H_2 evolution, suggesting a robust pH control chain in the bioreactors. Lastly, an experimental procedure to evaluate a theoretical reference yield of H_2 using glucose, taking into account the VFA as well as ethanol produced from the HPB microorganisms, was proposed and applied.

Appendix

Macro-approach and Relaxation Time

A so called *macro-approach* is a description of a complex system using the parameters which can be measured in order to take into account the observable behavior of the system. As the complexity of a system increases, the numbers of differential equations required to describe it grow. The systems encountered in biotechnology as well as in many of the engineering disciplines are of a complex nature and a rigorous description of their behavior leads to large sets of mathematical expressions (the *state equations*) describing the time evolution of a large number of relevant variables (the *state variables*). These equations generally contain a massive number of parameters, which in most cases cannot be readily obtained experimentally. Hence a consistent approach must be developed to simplify the picture of reality to a less complex one which can still describe the aspects of behaviour that are relevant to the desired application with sufficient accuracy. A useful approach to such simplification can be based on an analysis of the internal mechanisms of a system and their so-called *relaxation times.*

When considering a system in contact with an environment and exchanging matter and energy with it, a specific number of intensive quantities at its boundary need to be considered, e.g. concentrations of a number of chemical substances, temperature and pressure. After a sufficiently long time, all the processes of the system will have reached rates which no longer change with time, i.e. the state of the system has become time-independent. This state can be of two different types:

- The system finally reaches a state of *thermodynamic equilibrium;* if this occurs the final rates of the internal processes become zero, i.e. a lack of phenomena.
- The system reaches a so-called *steady-state* in which internal processes with a non-zero rate may still take place. In fact, if this system reaches a different state

from thermodynamic equilibrium, at least one internal process must have a non-zero rate, whether or not a stationary state can exist. Depending on the magnitude of the dynamics of the system, this can be considered a pseudo-steady state or an "evolutionary" system which can move towards stable or unstable conditions.

Following Röels (1983) [30], a time-scale separation approach or *relaxation time* approach is followed, to reduce the description of the dynamics of the system without losing its validity in accordance with the desired applications. In simple words this approach considers, as affecting the dynamics of a phenomenon, only those mechanisms which present a relaxation time of the same order of magnitude independent of whether the phenomenon is internal to the system or belongs to the environment. The relaxation time must not be confused with the intrinsic constant of a different dynamic phenomenon. It represents the dynamics of interaction between the system and its surrounding environment. A brief mathematics is shown to clarify the concept. Considering a first-order system, there is a constant of proportionality between a flux and a driving force:

$$J = k\Delta F \tag{A.1}$$

the relaxation time is

$$\tau_r = 1/k \tag{A.2}$$

but unfortunately first-order systems rarely describe the dynamics of the real world. The kinetics of a biosystem or a more complex system may be described by:

$$r = f(M) \tag{A.3}$$

in which f is not a first-order relationship, and hence the relaxation time of the observed mechanism cannot be rigorously defined. A way to overcome this difficulty is to define a relaxation time that depends on the actual values of the space parameters. Linearizing Eq. (A.3), it follows that:

$$r = \frac{f(M)}{\prod_{i=1,n} M_i^{1/n}} \prod_{i=1,n} M_i^{1/n} \tag{A.4}$$

and the relaxation time for the j-th situation is:

$$\tau_{rj} = \frac{\prod_{i=1,n} M_i^{1/n}}{r_j} \tag{A.5}$$

where M_i is the i-th state variable and r_j is the *probe parameter*, i.e. the experimentally valued parameter to follow the dynamics of the phenomena selected in accordance with the purpose of the study and the available experimental

instrumentation. Equation (A.5) means that for a non-linear system it is possible to introduce the concept of *actual relaxation time* in the sense that it gives the time to reach a fraction (1 – 1/e) of the difference between the actual state (thermodynamic equilibrium or steady-state) and a new one as a consequence of change of matter and/or energy between the environment and the system which determines the dynamics. The rate and magnitude of exchange of matter and energy between system and environment determine the dynamics of the system towards a new stable or unstable state.

Application to First-Order Kinetics

The following simple example is intended to clarify the approach. Consider a well-stirred reactor in which a first-order chemical reaction takes place. Into the system a substrate solution of concentration C_{s0} is introduced at a rate F. The volume of the system V is considered constant and no volume generation is assumed to take place (note that, in the case of a microorganism population, this is not a valid assumption!). The concentration of the substrate in the flow leaving the system is assumed equal to the substrate concentration in the system (ideal mixing hypothesis). The following kinetic equation is assumed to specify the rate of the first-order process inside the system:

$$r = kC_{si} \tag{A.6}$$

in which r is the rate of the system evolution per unit of volume, k is the kinetic constant and C_{si} is the substrate concentration inside the system. The following balance equation describes the dynamics of the substrate concentration in the system as a CSTR (continuous stirred tank reactor):

$$\frac{\mathrm{d}C_{si}}{\mathrm{d}t} = {}^{F}/_{V}(C_{s0} - C_{si}) - KC_{si} \tag{A.7}$$

where C_{s0} is the inlet concentration. In a stationary state or steady-state the left-hand side vanishes, hence:

$$C_{ssi} = FC_{s0}/(F + kV) \tag{A.8}$$

Thus the following expression describes the rate of reaction in a stationary state:

$$r = kFC_{s0}/(F + kV) \tag{A.9}$$

The rate of reaction is expressed in quantities which can be externally measured (macro-parameters), e.g. the system volume V, the substrate concentration in the feed

solution C_{s0}, the flow rate F and through knowledge of such intensive parameters as the kinetic constant k of the system. The actual substrate concentration inside the system C_{si} does not appear. Considering a situation in which at a given moment in time the substrate concentration in the inlet is shifted from C_{s0} to C_{se}, the following differential equation describes the system's behaviour during the transient:

$$V\frac{\mathrm{d}C_{si}^{'}}{\mathrm{d}t} = F(C_{s0} - C_{si}^{'}) - kC_{si}^{'}V \tag{A.10}$$

with the initial condition:

$$C_{ssi} = FC_{s0}/(F + kV) \tag{A.11}$$

Hence the dynamics of the system is the solution of the equation (A.10), in the time domain:

$$C_{si} = \frac{(F/V)}{(F/V) + k}[C_{se} + (C_{s0} - C_{se})\exp\{-(F/V + k)t\}] \tag{A.12}$$

The concentration C_{si} increases asymptotically to its new steady-state value. The relaxation time is defined as the time which elapses before the difference between C_{si} and its initial steady-state value reaches a fraction (1 – 1/e) of the difference between the old and the new steady-state value, which in this case is given by:

$$\tau_R = 1/(F/V + k) \tag{A.13}$$

The relaxation time contains two contributions: the relaxation time *V/F* is the characteristic residence time in the reactor and $1/k$ is the relaxation time of the chemical reaction taking place. The last equation can be written as:

$$1/\tau_R = 1/\tau_1 + 1/\tau_2 \tag{A.14}$$

From it one can argue that the relative numerical value of the relaxation time determines the behaviour of the system: if the permanence time in the reactor is larger than the relaxation time of the system, the system dynamics is similar of that of a batch reactor (thermodynamic equilibrium will be reached); on the contrary, when the permanence time is less than the relaxation time of the system, the system evolves to reach a concentration equal to that of the feed, i.e. the reaction disappears. Only if the values are of the same order of magnitude there will be such an interaction between the system and the environment (Deborah number equal $\sim$ 1). In the second case the evolution of the system is governed only by the permanence time:

$$C_{si} = C_{se} + (C_{s0} - C_{se})\exp\{-(F/V)t\} \tag{A.15}$$

As one can see, this dynamic equation is a simpler one describing the behaviour of the system than equation (A.12).

Major details can be found in:

J.A. Röels, "*Energetic and kinetics in biotechnology*", Elsevier Biomedical Press, Amsterdam (1983)

C. Ouwerker, "*Theory of Macroscopic System*", Springer Verlag, Berlin (1991).

References

1. M.H. Zwietering, I. Jongernburger, F.M. Rombouts, K.V. Riet, Modeling of the bacterial growth curve. Appl. Environ. Microbiol. **56**(6), 1875–1881 (1990)
2. B. Gombertz, On the nature of the function expressive of the law of human mortality, and on a mode of determining the value of life contingencies. Philos. Trans. R. Soc. Lond. **115**, 513–585 (1825)
3. F.J. Richards, A flexible growth function for empirical use. J. Exp. Bot. **10**, 290–300 (1959)
4. C.J. Stannard, A.P. Williams, P.A. Gibbs, Temperature/growth relationship for psychotrophic food-spoilage bacteria. Food Microbiol. **2**, 115–122 (1985)
5. W.E. Ricker, Growth rates and models. Fish Physiol. **8**, 677–743 (1979)
6. Y. Mu, H.Q. Yu, G. Wang, Evaluation of three methods for enriching H_2-producing cultures from anaerobic sludge. Enzyme Microb. Technol. **40**(4), 947–953 (2006)
7. A.M. Gibson, N. Bratchell, T.A. Roberts, The effect of sodium chloride and temperature on the rate and extent of growth of Clostridium botulinum type A in pasteurized pork slurry. J. Appl. Bacteriol. **62**, 479–490 (1987)
8. E.M.T. EI-Mansi, C.F.A. Bryce, *Fermentation Microbiology and Biotechnology* (Taylor & Francis Press, London, 1999)
9. M. Soto, R. Mendez, J.M. Lema, Methanogenic and non-methanogenic activity tests. Theoretical basis and experimental set-up. Water Res. **27**(8), 1361–1376 (1993)
10. D.E. Contois, Kinetics of bacterial growth: relationship between population density and specific growth rate of continuous cultures. J. Gen. Microbiol. **21**, 40–50 (1959)
11. J.F. Andrews, *A Dynamic Model of the Anaerobic Digestion Process* (Department of Environmental Systems Engineering, Clemson University, Clemson, 1968), p. 52
12. R.H. Heyes, R.J. Hall, Anaerobic digestion modelling—the role of H_2. Biotechnol. Lett. **3**(8), 431–436 (1981)
13. F.E. Mosey, Mathematical modelling of short-chain volatile acids from glucose. Water Sci. Technol. **15**, 209–232 (1983)
14. G. Lyberatos, I.V. Skiadas, Modelling of anaerobic digestion—a review. Global Nest. Int. J. **1**(2), 63–76 (1999)
15. J. Wang, W. Wan, Kinetic models for fermentative hydrogen production: a review. Int. J. Hydrogen Energy **34**, 3313–3323 (2009)
16. H.P.F. Fang, C. Li, T. Zhang, Acidophilic biohydrogen production from rice slurry. Int. J. Hydrogen Energy **31**, 683–692 (2006)
17. J.E. Bailey, D.F. Ollis, *Biochemical Engineering Fundamentals*, 2nd edn. (McGraw & Hill Press, New York, 1986)
18. X. Chen, Y. Sun, Z. Xiu, X. Li, D. Zhang, Stoichiometric analysis of biological hydrogen production by fermentative bacteria. Int. J. Hydrogen Energy **31**, 539–549 (2006)
19. P.M. Vignais, B. Billond, J. Mayer, Classification and phylogeny of hydrogenase. FEMS Microbiol. Rev. **25**, 455–501 (2001)

20. M.W.W. Adams, L.E. Mortenson, J.S. Chen, Hydrogenase. Biochimica Biophysica Acta **594**, 105–116 (1981)
21. R. Cammack, K.K. Rao, C.P. Bargeron, K.G. Hutson, P.W. Andrew, L.J. Rogers, Midpoint redox potentials of plant and algal ferrodoxins. Biochem. J. **168**, 205–209 (1977)
22. K. Uyeda, J.C. Rabinowitz, Pyruvate-ferrodoxin oxidoreductase. IV studies on the reaction. J. Biol. Chem. **246**, 3120–3125 (1971)
23. C.Y. Lin, C.H. Lay, Carbon/nitrogen-ratio effect on fermentative hydrogen production by mixed microflora. Int. J. Hydrogen Energy **29**, 41–45 (2004)
24. A.M.S. Vieira, R. Bergamasco, M.L. Gimenes, C.V. Nakamura, B.P. Diasfilho, Enumeration and isolation of facultative anaerobic bacteria in an upflow anaerobic sludge blanket reactor treating wastewater from gelatine industry. Acta Scientiarium Biol. Sci. **25**(2), 257–260 (2003)
25. W.M. Chen, Z.J. Tseng, K.S. Lee, J.S. Chang, Fermentative hydrogen production with Clostridium butyricum CGS5 isolated from anaerobic sewage sludge. Int. J. Hydrogen Energy **30**, 1063–1070 (2005)
26. J.S. Chen, D.K. Blanchard, Isolation and properties of a unidirectional H_2-oxidizing hydrogenase from the strictly anaerobic N_2-fixing bacterium Clostridium pasterianum W5. Biochem. Biophys. Res. Commun. **84**, 1144–1150 (1978)
27. M.W.W. Adams, L.E. Mortenson, The physical and catalytic properties of hydrogenase II of Clostridium pasteurianum. J. Biol. Chem. **295**(11), 7045–7055 (1984)
28. B. Ruggeri, G. Sassi, On the modelling approach of biomass behaviour in bioreactor. Chem. Eng. Commun. **122**, 1–56 (1993)
29. B. Ruggeri, G. Sassi, V. Specchia, A holistic view of (Bio)kinetics. Chem. Eng. Sci. **24**, 4121–4132 (1994)
30. J.A. Röels, *Energetics and Kinetics in Biotechnology* (Elsevier Biomedical Press, Amsterdam, 1982)
31. L. Zadeh, Fuzzy sets. Inf. Control **8**, 338–353 (1965)
32. I. Hussy, F.R. Hawkes, R. Dinsdale, D.L. Hawkes, Continuous fermentative hydrogen production from wheat starch co-product by mixed microflora. Biotechnol. Bioeng. **84**(6), 619–626 (2003)